Journal of Applied and Computational Mechanics, Vol. 1, No. 3, (2015), 152-160
DOI: 10.22055/jacm.2015.11076


Journal of
Applied and Computational Mechanics

# Helicopter Blade Stability Analysis Using Aeroelastic Frequency Response Functions

**Mostafa Mohagheghi[1], Ali Salehzadeh Nobari[2], Seyed Alireza Seyed Roknizadeh[3]**

[1] PhD candidate, Faculty of New Sciences and Technology, University of Tehran
North Kargar St, Tehran, 14395-1561, Iran, Mo.mohagheghi@ut.ac.ir,

[2] Professor, Department of Aerospace Engineering, Amirkabir University of Technology
Hafez St, Tehran, 15875-4413, Iran, andishan.pars@gmail.com

[3] Assistant Professor, Engineering Faculty, Department of Mechanical Engineering, Shahid Chamran University of Ahwaz
Golestan Boulevard, Ahvaz, 61357-83151, Iran, s.roknizadeh@scu.ac.ir

Received: November 03 2014; revised March 02 2015; accepted for publication April 09 2015.
Corresponding author: Mo.mohagheghi@ut.ac.ir.

**Abstract**

In the present paper, the aeroelastic stability of helicopter rotor blade is determined using Aeroelastic Frequency Response Function. The conventional methods of aeroelastic stability usually use an iterative procedure while the present method does not require such approach. Aeroelastic Frequency Response Functions are obtained by inverting dynamic stiffness matrix of the aeroelastic system. System response could be obtained through exciting each degree of freedom. The resulting response was then plotted and the behavior of this function was investigated to find out the stability criteria and system natural frequencies. The results of this method are compared with stability boundaries obtained from the conventional p-k method and it can be inferred that, compared to other methods, the present algorithm is of less numerical cost.

**Keywords**: Aeroelastic Frequency Response Function, Helicopter blade, Loewy unsteady aerodynamic theory.

## 1. Introduction

Aeroelastic stability is one of the main concerns in the design of aircraft wings and helicopter blades. For stability investigations there are conventional methods which can be broadly divided into two categories, namely, time domain methods and frequency domain methods. The computational solution of the governing equations and the determining of the system stability constitute one of the common approaches in the time domain method. Aeroelastic modeling and stability investigation in the frequency domain is another approach, which does not require time integrals. In addition to this advantage, the circulatory parts of aerodynamic terms are distinguishable from non-circulatory terms. Root locus analysis and p-k method are also two conventional procedures for determining system stability. P-k method is an iterative solution for unsteady aeroelastic models while the root locus is more usual for quasi-steady models [1]. However, there are other methods for determining the stability of an aeroelastic system. For example, Imregun investigated the aeroelastic behavior of turbine blades in frequency domain by means of rational fraction analysis [2], applying 2D linearized cascade theories for aerodynamic modeling to predict the effect of elastic axis position on the turbine blade stability. Roknizadeh et al. analyzed the aeroelastic stability of a system using FRF and condition number [3]. In their work, a quasi-steady aerodynamic model was used for blade analysis.

In the present study, the aeroelastic stability of helicopter rotor blade is determined using unsteady aerodynamic model and aeroelastic frequency response functions. The results are validated through p-k method. Indeed, in this paper the emphasis is on the solution method rather than modeling complexity of system.

## 2. Frequency Response Function

Generally, FRF[1] is a frequency dependent transfer function. One of the most frequently used shapes of FRF is receptance which represents the response of a system due to an applied harmonic force. FRF is one of the most important tools for vibration analysis.

In Multi Degree of Freedom systems, the characteristics of the system can be described by a matrix, known as frequency response matrix [H( $\omega$ )]. Each element of this matrix is a FRF. In fact, $H_{ij}(\omega)$ is the harmonic response $x_i$, in one degree of freedom i, caused by a harmonic force $F_j$ applied at a different DOF[2], j [4]. In this article, the FRF matrix is obtained by inverting dynamic stiffness matrix. The procedure of calculations is presented in the next parts.

## 3. Aeroelastic Model

For structural modeling, the nonlinear Euler-Bernoulli beam theory is applied [5, 6] which considers centrifugal forces and which was developed by Hodges-Dowel. This is a common model for helicopter blade aeroelastic analysis and has been used in some previous works [7-10]. However, in these works, the aerodynamic model is based on Greenberg's extension of Theodorsen's theory. Shahverdi performed the aeroelastic blade analysis with reduced order aerodynamic model, using this structural model of blade [7]. He also derived the formulation for rotor blade with unsteady aerodynamic in the frequency domain.

As can be seen from Fig. 1, in the mentioned structural model elastic displacements in x, y and z directions are denoted by u, v and w. Moreover, the elastic twist of blade about x axis is represented by $\varphi$ while $\theta$ is the blade pitch angle. Therefore, the angle of blade section with respect to rotor disc equals to $\varphi+\theta$. In the considered model chord wise offsets between center of mass, elastic center and aerodynamic center is assumed to be zero.

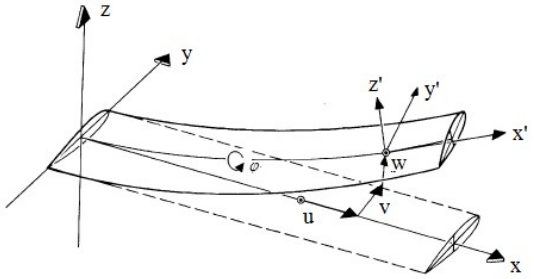


**Fig. 1.** Elastic displacements of the blade

The aerodynamic lift and pitching moment for the blade in hover is calculated by using Loewy aerodynamic theory. Loewy considered the effects of spiral wake beneath the rotor and revised Theodorsen theory, which had been presented for pulsating airfoil in incompressible flow. The Loewy lift deficiency function is [11,12]:

$$C'(k)=\frac{H_1^{(2)}+2J_1W}{H_1^{(2)}+iH_0^{(2)}+2(J_1+iJ_0)W} \tag{1}$$

where W is the wake weighting function defined as [7]:

$$W=\frac{1}{e^{\frac{4\bar{V}_i}{\sigma}}.e^{\frac{i2\pi\omega}{\Omega N_b}}-1}=\frac{1}{e^{\frac{4\bar{V}_i}{\sigma}}.e^{\frac{i3k}{\sigma}}-1} \tag{2}$$

and $\bar{V}_i$, $\sigma$, $N_b$ and k are non-dimensional induced velocity, blade solidity, number of blades and reduced frequency, respectively. Finally, substituting aerodynamic forces into structural equations, we obtain the following non-dimensional relations for in-plane bending, out-plane bending and torsion of blade:

$$\begin{aligned}
&-\frac{\mu^2K}{2}\left[\left(1-\bar{x}^2\right)\phi'\right]-\kappa\phi''+\frac{\gamma\bar{c}^{-2}}{48}\bar{x}\dot{\varphi}+\mu^2\ddot{\varphi}\\
&+\left(\Lambda_2-\Lambda_1\right)\left[\left(\frac{\bar{w}''^2-\bar{v}''^2}{2}\right)\sin(2\theta)+\bar{v}''\bar{w}''\cos(2\theta)\right]\\
&+\left(\mu_2^2-\mu_1^2\right)\varphi\cos(2\theta)=-\left(\mu_2^2-\mu_1^2\right)\frac{\sin(2\theta)}{2}\\
&+\bar{F}e^{i\omega t}\delta(\bar{x}-\bar{x}_0)
\end{aligned} \tag{3}$$

[1] . Frequency Response Function
[2] . Degree Of Freedom

$$
\begin{aligned}
&-\left[\bar{v}'\int_{\bar{x}}^{1}(\bar{x}+2\dot{\bar{v}})d\bar{x}\right]'+\left(\Lambda_2-(\Lambda_2-\Lambda_1)\sin^2(\theta)\right)\bar{v}''''\\
&+\frac{(\Lambda_2-\Lambda_1)\sin(2\theta)}{2}\bar{w}''''-2\int_{0}^{\bar{x}}(\bar{v}'\dot{\bar{v}}'+\bar{w}'\dot{\bar{w}}')d\bar{x}+\ddot{\bar{v}}-\bar{v}\\
&+(\Lambda_2-\Lambda_1)\left[-\sin(2\theta)(\phi\bar{v}'')''+\cos(2\theta)(\phi\bar{w}'')''\right]\\
&+\frac{\gamma}{6}\begin{Bmatrix}C'(k)\overline{xV_i}\varphi+\left[\frac{2C_{d_0}}{C_{l\alpha}}\bar{x}+C'(k)(\theta+\varphi)\overline{V_i}\right]\dot{\bar{v}}\\-C'(k)\left[2\overline{V_i}-\bar{x}(\theta+\varphi)\overline{V_i}\right]\bar{w}\end{Bmatrix}\\
&=\frac{\gamma}{6}\left(C'(k)\overline{V_i}^2-\frac{C_{d_0}}{C_{l\alpha}}\bar{x}^2-C'(k)\overline{xV_i}\theta\right)+\bar{F}e^{i\omega t}\delta(\bar{x}-\bar{x}_0)
\end{aligned}
\tag{4}
$$

$$
\begin{aligned}
&-\left[\bar{w}'\int_{\bar{x}}^{1}(\bar{x}+2\dot{\bar{v}})d\bar{x}\right]'+\Lambda_1\bar{w}''''+(\Lambda_2-\Lambda_1)\sin^2(\theta)\bar{w}''''+\\
&+\frac{(\Lambda_2-\Lambda_1)\sin(2\theta)}{2}\bar{v}''''+(\Lambda_2-\Lambda_1)\left[\cos(2\theta)(\phi\bar{v}'')''+\sin(2\theta)(\phi\bar{w}'')''\right]\\
&+\bar{w}(1+\frac{\gamma\bar{c}}{24})\\
&+\frac{\gamma}{6}C'(k)\begin{Bmatrix}-\bar{x}^2\left(\varphi+\int_{0}^{\bar{x}}(\bar{v}'\bar{w}'')d\bar{x}\right)+\overline{xvw}'-\frac{\bar{c}}{2}\overline{xw}'-\left[2\bar{x}(\theta+\varphi)-\overline{V_i}\right]\dot{\bar{v}}\\+\bar{x}\dot{\bar{w}}-\frac{\bar{c}}{2}\left(\frac{1}{2}+C'(k)\right)\bar{x}\dot{\varphi}\end{Bmatrix}\\
&=\frac{\gamma}{6}C'(k)\left(-\overline{xV_i}+\bar{x}^2\theta\right)+\bar{F}e^{i\omega t}\delta(\bar{x}-\bar{x}0)
\end{aligned}
\tag{5}
$$

In the above equations, a harmonic excitation has been considered on the blade in order to determine system FRF and denoted by $\bar{F}e^{i\omega t}\delta(\bar{x}-\bar{x}_0)$. $\bar{x}_0$ is the location of applied excitation force (or moment) at the blade section and is considered at the end of blade, i. e. $\bar{x}_0=1$. In the final equations (eqs. 13-14), the excitation forces in y and z directions are shown by index of 1 and 2, respectively. Also, the index 3 for $\bar{F}$ represents the excitation pitching moment.

Now, these nonlinear integro-partial differential equations are reduced to a set of ordinary differential equations by Galerkin method. To this end, the non-dimensional elastic displacements are estimated as [6]:

$$\bar{V}=\sum_{j=1}^{6}V_j\Psi_j(\bar{x}) \tag{6}$$

$$\bar{w}=\sum_{j=1}^{6}W_j\Psi_j(\bar{x}) \tag{7}$$

$$\bar{\varphi}=\sum_{j=1}^{6}\phi_j\theta_j(\bar{x}) \tag{8}$$

Where $V_j$, $W_j$ and $\phi_j$ are generalized coordinates and $\Psi_j(\bar{x})$ and $\theta_j(\bar{x})$ are bending and torsional mode shapes of a cantilevered beam, respectively. In this study, 6 mode shapes are considered for each d.o.f. Thus, 18 nonlinear ordinary differential equations are obtained after Galerkin method is applied. Nevertheless, linear equations are necessary for calculating the aeroelastic frequency response function (AFRF). Therefore, linearization about static equilibrium condition ($V_0, W_0, \phi_0$) is performed which results in the following general form:

$$[M]\{\ddot{q}\}+[C]\{\dot{q}\}+[K]\{q\}=\{F\} \tag{9}$$

where q is the variation of generalized coordinate vector about equilibrium condition and contains 18 rows:

$$\{q\}=\begin{Bmatrix}\Delta V_j\\ \Delta W_j\\ \Delta\phi_j\end{Bmatrix}_{18\times1} \tag{10}$$

Also, M, C and K are mass, damping and stiffness matrices, which consist of structural and aerodynamic parts, and are as follows:

$$M_s=\begin{bmatrix}\delta_{ij} & 0 & 0\\ 0 & \delta_{ij} & 0\\ 0 & 0 & \mu^2\delta_{ij}\end{bmatrix},\ M_a=\begin{bmatrix}0 & 0 & 0\\ 0 & \delta_{ij}\dfrac{\gamma\bar{c}}{24} & 0\\ 0 & 0 & 0\end{bmatrix} \tag{11}$$

$$C_s=2\begin{bmatrix}\sum_{k=1}^{6}(F_{ikj}-F_{jki})V_{0k} & \sum_{k=1}^{6}(F_{jki})W_{0k} & 0\\ \sum_{k=1}^{6}(F_{jki})W_{0k} & 0 & 0\\ 0 & 0 & 0\end{bmatrix} \tag{12}$$

$$K_{s_{13}}=(\Lambda_2-\Lambda_1)\sum_{k=1}^{6}K_{jki}\left[-V_{0k}\sin(2\theta)+W_{0k}\cos(2\theta)\right] \tag{13}$$

$$\begin{aligned}K_{s_{22}}&=D_{ij}+\left[\Lambda_1-(\Lambda_2-\Lambda_1)\sin^2\theta\right]\beta_j^4\delta_{ij}\\&\quad+(\Lambda_2-\Lambda_1)\sum_{k=1}^{6}K_{kji}\phi_{0k}\sin(2\theta)\end{aligned} \tag{14}$$

$$K_{S23}=(\Lambda_2-\Lambda_1)\sum_{k=1}^{6}K_{jki}\varphi_{0j}\left[V_{0k}\cos(2\theta)+W_{0k}\sin(2\theta)\right] \tag{15}$$

$$K_{s_{31}}=(\Lambda_2-\Lambda_1)\sum_{k=1}^{6}K_{ijk}\left[-V_{0k}\sin(2\theta)+W_{0k}\cos(2\theta)\right] \tag{16}$$

$$K_{s_{32}}=(\Lambda_2-\Lambda_1)\sum_{k=1}^{6}K_{ijk}\left[V_{0k}\cos(2\theta)+W_{0k}\sin(2\theta)\right] \tag{17}$$

$$K_{s_{33}}=\mu^2KN_{ij}+\left[\kappa\gamma_j^2+\left(\mu_2^2-\mu_1^2\right)\cos(2\theta)\right]\delta_{ij} \tag{18}$$

$$K_{s_{21}}=K_{s_{12}} \tag{19}$$

$$K_a=\frac{\gamma C'(k)}{6}\begin{bmatrix}0 & 0 & \overline{V}_iI_{ij}\\ \sum_{k=1}^{6}L_{ijk}W_{0k} & -\dfrac{\bar{c}}{2}O_{ij}+\sum_{k=1}^{6}L_{ikj}V_{0k} & -J_{ij}\\ 0 & 0 & 0\end{bmatrix} \tag{20}$$

In addition, minimizing the error of last terms of eqs. (3-5) yields:

$$\begin{aligned}\{F\}_{18\times1}=\overline{F_j}\,e^{i\omega t}<&\ \Psi_1(1)\ \Psi_2(1)\ \Psi_3(1)\ \Psi_4(1)\\&\Psi_5(1)\ \Psi_6(1)\ \Psi_1(1)\ \Psi_2(1)\ \Psi_3(1)\ \Psi_4(1)\ \Psi_5(1)\ \Psi_6(1)\\&\theta_1(1)\ \theta_2(1)\ \theta_3(1)\ \theta_4(1)\ \theta_5(1)\ \theta_6(1)>^T\end{aligned} \tag{21}$$

Because of harmonic excitation, the following harmonic response is assumed:

$$\{q\}=\begin{Bmatrix}\overline{\Delta V_j}\\ \overline{\Delta W_j}\\ \overline{\Delta\phi_j}\end{Bmatrix}e^{i\omega t} \tag{22}$$

Thus, eq. (9) becomes:

$$\left(-\omega^2[M]+i\omega[C]+[K]\right)\begin{Bmatrix}\overline{\Delta V_j}\\ \overline{\Delta W_j}\\ \overline{\Delta\phi_j}\end{Bmatrix}=\begin{Bmatrix}\overline{F_1}\Psi_j(1)\\ \overline{F_2}\Psi_j(1)\\ \overline{F_3}\theta_j(1)\end{Bmatrix} \tag{23}$$

Hence, variation of generalized coordinates is:

$$\begin{Bmatrix} \overline{\Delta V_j} \\ \overline{\Delta W_j} \\ \overline{\Delta \phi_j} \end{Bmatrix} = \left( -\omega^2 [M] + i\omega [C] + [K] \right)^{-1} \begin{Bmatrix} \overline{F_1} \Psi_j(1) \\ \overline{F_2} \Psi_j(1) \\ \overline{F_3} \theta_j(1) \end{Bmatrix} \tag{24}$$

Frequency ( $\omega$ ) and blade pitch angle ( $\theta$ ), that is in $K$ matrix, are two variables of eq. (24). For each value of blade pitch angle, the mass and damping matrices can be evaluated to investigate the stability.

The other required parameters for achieving matrices are given in Table 1. The natural rotating frequencies $\omega_w$, $\omega_v$ and $\omega_\phi$ are obtained from Ref [13].

At this stage, once the excitation force at one of DOFs is applied, the generalized coordinates can be computed from eq. (24) and then using eqs. (6 - 8). The elastic displacements are 6 calculated as a function of frequency:

$$\overline{\Delta v} = \sum_{j=1}^{6} \overline{\Delta V_j} \Psi_j(\bar{x}) \tag{25}$$

$$\overline{\Delta w} = \sum_{j=1}^{6} \overline{\Delta W_j} \Psi_j(\bar{x}) \tag{26}$$

$$\overline{\Delta \varphi} = \sum_{j=1}^{6} \overline{\Delta \phi_j} \theta_j(\bar{x}) \tag{27}$$

It should be mentioned that by exciting each DOF three responses are obtained, which can be plotted against frequency. In the next sections, these curves are used to determine system stability criteria.

## 4. State space modeling for pk method solution

As presented previously, mass, damping and stiffness are reduced frequency dependent matrices and system stability cannot be determined by eigen value solution or p method. Thus, the p-k method is used to validate the results obtained from AFRF diagrams (the present method). In the p-k method, first, the coefficient matrices are calculated by an initial guess for frequency. Then, reduced frequencies are gained using imaginary parts of the coefficient matrix eigen values. In the second iteration, these reduced frequencies are substituted in the Loewy function and coefficient matrices are calculated again. This procedure continues until the difference between two consecutive frequencies becomes less than predetermined error value. In this step the stability is determined by considering the sign of real part of the eigen value. That is, if the real part is positive, the system becomes unstable. If low rate of decay of oscillations is taken into account, the aerodynamic response can be assumed to be harmonic with frequency k, while the structural response consists of both imaginary and real parts [1, 14].

To calculate 18 eigen values of the present system, we rewrite the equations in the standard format. Decoupling the general form of the governing equations yields:

$$(M_S + M_a)\ddot{q} + (C_S + C_a)\dot{q} + (K_S + K_a)q = 0 \tag{18}$$

Assuming harmonic response ( $q = \bar{q}e^{i\omega t}$ ) for aerodynamic part, we get:

$$(M_S\ddot{q} + C_S\dot{q}) + \left(-M_a\omega^2 + C_a i\omega + K_a + K_S\right)q = 0 \tag{19}$$

If the structural response by the form of $\bar{q}e^{Pt}$ is added, the above equation can be expressed as:

$$(M_S P\dot{q} + C_S Pq) + \left(-M_a\omega^2 + C_a i\omega + K_a + K_S\right)q = 0 \tag{20}$$

or in the matrix form:

$$\begin{bmatrix} M_S P & C_S P \\ 0 & -IP \end{bmatrix} \begin{Bmatrix} \dot{q} \\ q \end{Bmatrix} = -\begin{bmatrix} 0 & K_c \\ I & 0 \end{bmatrix} \begin{Bmatrix} \dot{q} \\ q \end{Bmatrix} \tag{21}$$

where

$$K_c = -M_a\omega^2 + C_a i\omega + K_a + K_S \tag{22}$$

and I is the identity matrix. After Eq. (21) is solved as an eigen value problem, 18 eigen values are attained:

$$p_i = \sigma_i + i\omega_i \tag{23}$$

After eigen values are arranged, lift deficiency function and hence coefficient matrices are calculated for each frequency (i.e. the imaginary part of eigen value) and new eigen values are obtained. Thus, in this step there are 18 arranged eigen value (e. v.) sets. The first e. v. of the first set is compared with the minimum e. v. of the previous step and n-th e. v. of n-th set is compared with corresponding eigen value. Thus, 18 differences resulted from 18 comparisons obtained. If the maximum value of these differences is greater than the permitted error (for example 0.0001), the previous eigen values are substituted with new ones and the procedure is repeated until it converges. After convergence, if the real part of at least one of eigen values is positive, the system is unstable and the whole procedure is finished.

## 5. Results

To investigate the aeroelastic behavior of the blade, variation of in-plane bending amplitude, which was obtained from eq. (15), is plotted in Fig. 2. Index 3 in $\Delta v_3$ shows that the excitation is applied at the pitch DOF (3rd DOF). This figure has been obtained for the blade pitch angle of 0.333 rad which is the critical pitch angle according to p-k method. Each peak of AFRF curve indicates a natural frequency of the system. Because of considering 18 generalized coordinates, 18 peaks are expected. Note that in Fig. 2 the excitation is on the blade tip in the torsional mode and the response is predicted for in-plane bending. Also, frequency varies from 0 to 100 rad/sec and it does not include all the peaks. The global maximum of FRF occurs in 1.808 rad/sec.

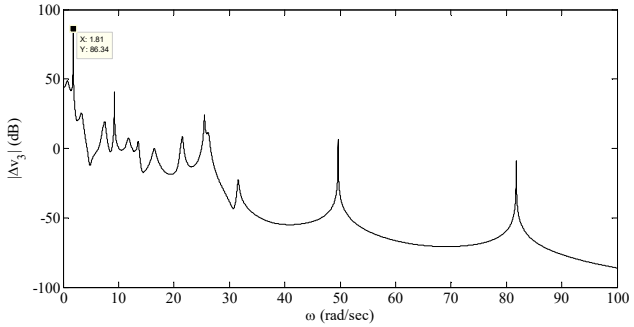


**Fig. 2.** The amplitude of AFRF at the critical pitch angle (frequency step: 0.01 rad/sec)

AFRF is then plotted in the neighbor of this frequency for 3 different values of blade pitch angle, i.e. $0.9\,\theta_{cr}$, $\theta_{cr}$ and $1.1\ \theta_{cr}$. As depicted in Fig. 3, the peak of AFRF at the critical angle is more than the peaks of smaller and larger angles. This behavior is due to damping variations. That is to say, at the beginning of instability, the damping of one mode becomes negative and hence the magnitude of damping at the critical angle reaches minimum value. Increasing pitch angle after occurring instability results in more negative damping and increases the value of terms in the denominator of AFRF. This leads to a decrease in calculated AFRF. A better presentation of this event is illustrated in Fig. 4 which shows the values of AFRF peaks for different blade pitch angles.

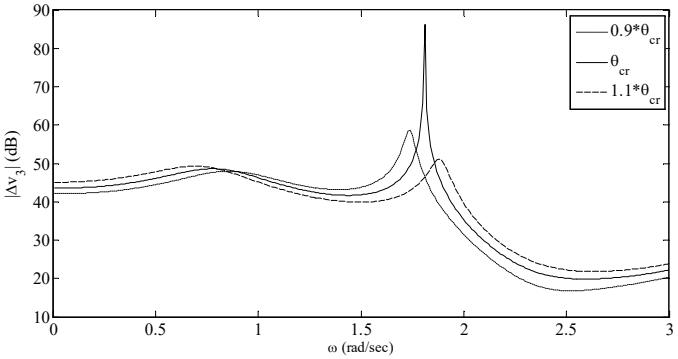


**Fig. 3.** AFRF for three different pitch angles (frequency step: 0.01 rad/sec)

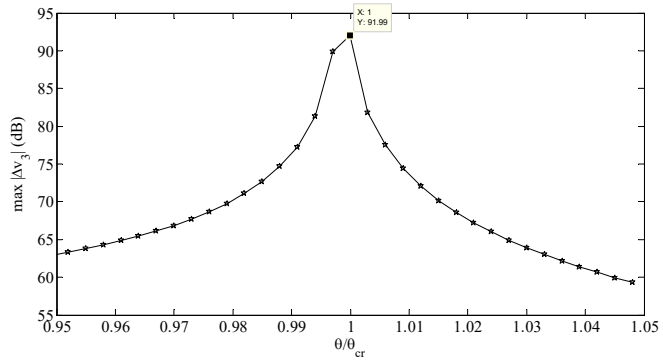


**Fig. 4.** Variation of $\Delta v_3$ peaks (frequency step: 0.001 rad/sec)

The same graph for amplitude of out-plane bending ($\Delta w$) duo to the unique excitation on the in-plane DOF is plotted in Fig. 5 for another blade. The structural characteristics of this blade are given in table 2.

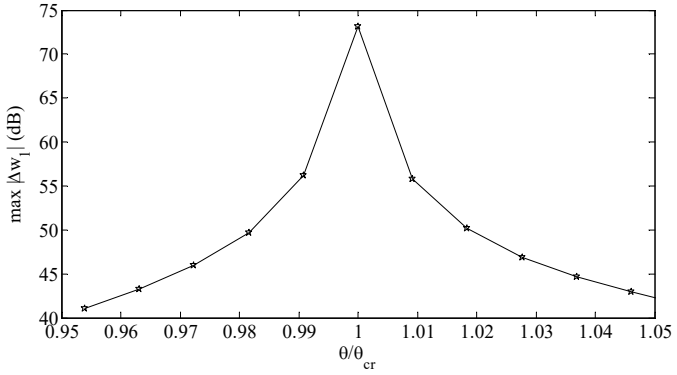


**Fig. 5.** The variation of $\Delta\phi_2$ peaks for blade 2 (frequency step: 0.001 rad/sec)

The behavior of this blade is the same as that of the first one and in the instability pitch angle it riches its maximum value.

In addition, as noted before, the peaks of AFRF correspond to the natural frequencies of the system. Figure 6 shows the AFRF peaks at the critical pitch angle and can be compared with natural frequencies in Table 3 obtained through p-k method.

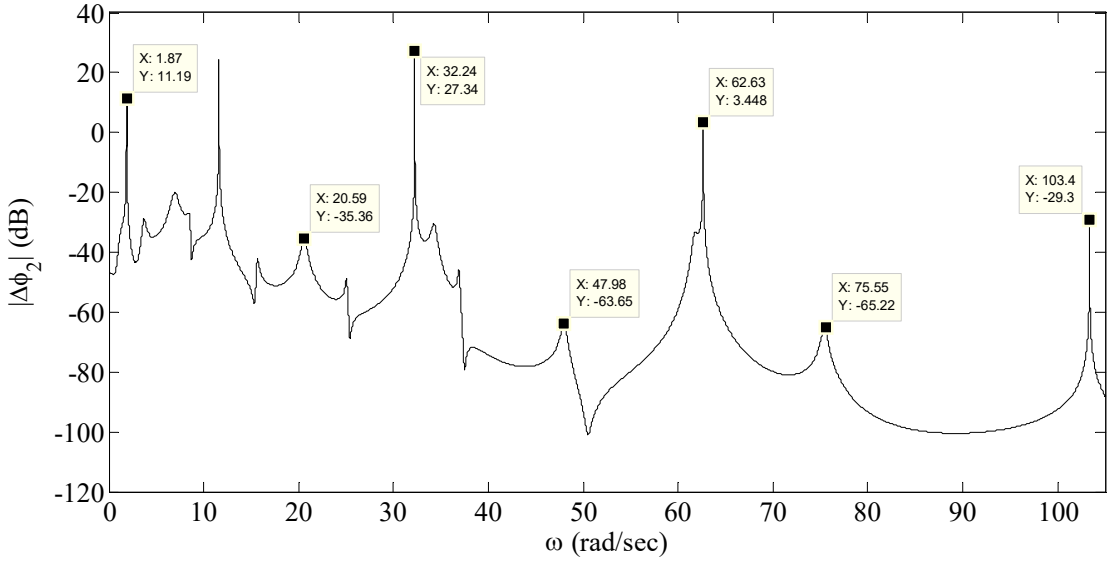


**Fig. 6.** The amplitude of AFRF at the critical pitch angle for blade 2

## 6. Conclusion

In this study, the behavior of an aeroelastic system (rotor blade) was investigated via AFRF diagram. For this purpose, rotor blade was modeled as a nonlinear Euler-Bernouli beam and the critical pitch angle was determined by applying the conventional p-k method. AFRF was then obtained and plotted for different pitch angles. As expected, it was seen that the peak of AFRF amplitude becomes maximum in $\theta_{cr}$ and this behavior of AFRF could be used as an alternative method in the determination of system stability boundaries. One of the advantages to this method is eliminating iteration for converging reduced frequency. Also, other modal characteristics such as natural frequencies can be obtained from AFRF diagrams. However, it should be noted that the phase diagram of AFRF does not include this information.

The results indicated that although instability pitch angle in quasi-steady and unsteady assumptions are notably different, the frequencies of instability are approximately the same. Thus, to save time, one can at first obtain the instability frequency from quasi-steady analysis and then determine the more accurate critical pitch angle by investigating unsteady AFRF diagram in the neighbor of that frequency.

## Nomenclature

| | | | |
|---|---|---|---|
| *Ai-Oij* | Modal integrals [-] | $\gamma$ | Lock number ( $\gamma = 3\rho_\infty c l_\alpha c R / m$ ) [-] |
| *c* | Blade chord [m] | $\delta_{ij}$ | Kronecker delta [-] |
| *C'(k)* | Loewy's lift deficiency function [-] | $\theta_{cr}$ | Critical pitch angle |
| *F* | Excitation force [N] | $\kappa$ | Dimensionless torsional rigidity ( $\kappa = GJ / m\Omega^2 R^4$ ) [-] |
| *k* | Reduced frequency, $2c\omega / 3R\Omega$ [-] | $\Lambda_1, \Lambda_2$ | Dimensionless bending stiffnesses ( $\Lambda_1 = EI_1 / m\Omega^2 R^4$ ) [-] |
| *kA, km* | Blade cross-section polar and mass radius of gyration, respectively [m] | $\mu$ | Dimensionless mass radii of gyration [-] |
| *k* | kA2/ km2[-] | $\sigma$ | Solidity ( $N_b c / \pi R$ ) [-] |
| *Nb* | Number of blades [-] | $\varphi$ | Elastic torsion deflection [rad] |
| *q* | Vector of generalized coordinates [-] | $\Psi_j(\bar{x})$ | Bending and torsional mode shapes of a cantilevered beam [-] |
| *R* | Blade radius [m] | $\theta_j(\bar{x})$ | |
| *u, v, w* | Displacements in the x, y, z directions, respectively [m] | $\omega$ | Frequency [sec-1] |
| *x, y, z* | Undeformed coordinate system [m] | $\bar{(\ )}$ | Non-dimensional parameter ( /R or / $R\Omega$ ) |

| | | | |
|---|---|---|---|
| $A_c$ | Cross-section area of micro-channel [m$^2$] | $T$ | Local mean temperature [K] |
| $L_x$ | Length of heat sink [m] | $U_i$ | Mean velocity components (i=1, 2, 3) |
| $R_{th}$ | Thermal resistance [ $^o$C/W] | $\theta$, $\phi$ | Design variables, $W_c/H_c$ and $W_w/H_c$ |

## References

[1]. Hassig H. J., "An Approximate True Damping Solution of the Flutter Equation by Determinant Iteration", Journal of Aircraft, 8(11), pp. 885-890, 1971.

[2]. Imregun M., "Prediction of Flutter Stability Using Aeroelastic Frequency Response Functions", Journal of Fluids and Structures, 9 (4), pp. 419-434, 1995.

[3]. Roknizadeh, S. A. S., "Stability Analysis of Aeroelastic Systems Based on Aeroelastic FRF and Condistion Number", Aircraft Engineering and Aerospace Technology, Vol. 84, No. 5, pp. 299-310, 2012.

[4]. Ewins D. J., Modal Testing: Theory, Practice and Application. 2Ed. Research Studies Press, Hertfordshire, England, 2000.

[5]. Hodges D. H. and Dowell E. H., "Nonlinear Equations of Motion for the Elastic Bending and Torsion of Twisted Nonuniform Rotor Blades", NASA TN D-7818, 1974.

[6]. Hodges D. H. and Ormiston R. A., "Stability of Elastic Bending and Torsion of Uniform Cantilever Rotor Blades in Hover with Variable Structural Coupling", NASA TN D-8192, 1976.

[7]. Shahverdi H., "Aeroelastic Analysis of Helicopter Rotor Blades Using Reduced Order Aerodynamic Model", Ph. D. Dissertation, Amirkabir University of Technology, 2006.

[8]. Afagh F. F. and Nitzsche F. and Morozova N., "Dynamic Modeling and Stability of Hingeless Helicopter Blades with a Smart Spring", The Aeronautical Journal, 108 (1085), pp. 369-377, 2004.

[9]. Nariman M., "Vibration Computation of Helicopter Rotor Blades Using Unsteady Aerodynamic Theory", M.Sc. Thesis, Amirkabir University of Technology, 2007.

[10]. Gennaretti M. and Molica Colella M. and Bernardini G., "Analysis of Helicopter Vibratory Hub Loads

Allevation by Cyclic Trailing-edge Blade Flap Actuation", The Aeronautical Journal, 113 (1146), pp. 549-556, 2009.
[11]. Johnson W., Helicopter Theory, Princeton University Press, New Jersey, 1980.
[12]. Bielawa R. L., Rotary Wing Structural Dynamics and Aeroelasticity, AIAA Inc., Washington, 1992.
[13]. Sotoodeh Z., "Aeroelastic Analysis of Helicopter Cantilever Rotor Blade with Piters-Hey Induced Flow Model in Hover", M.Sc. Thesis, Sharif University of Technology, 2007.
[14]. Haddadpour H. and Firouz-Abadi R. D., "True Damping and Frequency Prediction for Aeroelastic Systems: The PP Method", Journal of Fluids and Structures, 25(7), pp. 1177-1188, 2009.